Journal of Materials Chemistry C

Accepted Manuscript

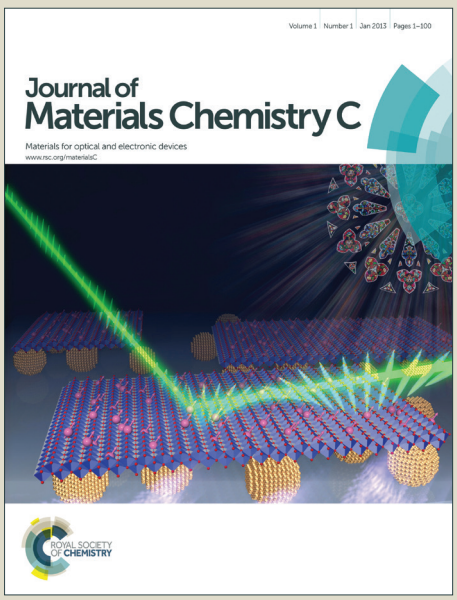

ROYAL SOCIETY OF CHEMISTRY

www.rsc.org/materialsC

Journal Name

RSCPublishing

ARTICLE

N,N'-Dihydrotetraazapentacenes (DHTA) in thin film transistors†

Cite this: DOI: 10.1039/xoxxoooooox

Fabian Paulus,[a] Benjamin D. Lindner,[a] Hilmar Reiß,[a] Frank Rominger,[a] Andreas Leineweber,[b] Yana Vaynzof,[c,d] Henning Sirringhaus[e] and Uwe H. F. Bunz[a,d]*

Received ooth January 2012,
Accepted ooth January 2012

DOI: 10.1039/xoxxoooooox

www.rsc.org/

The synthesis and structural properties of three *N,N'*-dihydrotetraazapentacenes (DHTA) are described. The different substitution pattern (H, F, Cl) of the dihydrotetraazapentacene body exhibited a significant effect on the optical, electronic and morphological properties of the derivatives in thin films. The synthesized materials were investigated as active layers in top gate/ bottom contact (BC/TG) transistors. The transistor performance of the dichlorinated derivative was almost independent on the processing conditions with an average hole mobility of ~0.04 cm²/Vs and best mobility values ranging from 0.07 to 0.11 cm²/Vs. Each of the three derivatives was found to exhibit an individual packing motif in solution grown crystals, determined by single crystal X-Ray analysis. Surprisingly, for all three materials a different polymorph formed in spin cast films explaining the observed morphology and FET performance.

Introduction

Over the last decade small molecules have proven to be useful semiconductors in solution processed organic field-effect transistors (OFET).[1,2] High mobility values (>1.0 cm²/Vs) for hole and electron transport have been reported, especially for acene based materials.[3–5] The introduction of triisopropyl-silylethynyl side chains, first reported by Anthony *et al.*, makes acenes solution processable.[6–8] It is commonly accepted that the molecular structure determines the intermolecular packing and interaction of the aromatic core units in the solid state.[8] The performance of small molecules in OFETs strictly depends on the interplay between molecular packing and the microstructure of their thin films. Nevertheless, detailed studies of acenes have shown that multiple crystal modifications (polymorphs) exist and a detailed study of the obtained films is necessary. For pentacene and rubrene polymorphs were reported by Dimitrakopoulos *et al.* and Kaefer *et al.*, respectively.[9–13] Each polymorph can exhibit different transport properties due to an altered π-π stacking of the aromatic units its solid state. Giri *et al.* show that 6,13-bis(triisopropyl)silyl-ethynylene pentacene (TIPS-Pen) forms non-equilibrium phases with different electrical properties, depending on the processing conditions of this soluble semiconductor.[14–16]

Azaacenes are a class of materials that have gained great interest as semiconducting materials when Nuckolls *et al.* first reported a thin film transistor with dihydrodiazapentacene (DHDAP) as active layer (Figure 1).[17–20]

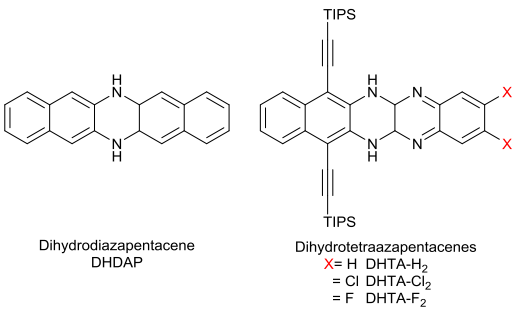

Fig. 1 Molecular structures of the semiconducting material from Nuckolls (left) and the three materials **DHTA-X₂** used in this study.[20]

DHDAP is an oxidation resistant small molecule and can be processed from polar, high boiling solvents such as dimethylformamide (DMF).[20] The material is a p-type semiconductor with reported mobilities of up to 0.45 cm²/Vs. Also, DHDAP exhibits different polymorphs in its solid state and the correct polymorph must be obtained for an optimum transistor performance.[21]

The results from Nuckolls and Miao suggest that reduced azaacenes are fundamentally attractive organic semiconductors with a significant potential for application in organic electronics.[20,22,23] We have recently developed a powerful synthetic route towards differentially substituted di- and tetraazaacenes.[24] Here we describe the OFET performance for three substituted, consanguine *N,N'*-dihydrotetraazapentacenes (**DHTA-H₂, DHTA-Cl₂, DHTA-F₂**). These reduced azaacenes are easily produced and show attractive, substituent dependent

hole transport properties (up to 0.1 cm²/Vs). We analysed the crystal packing and microstructure of those materials to understand and correlate the molecular structure with their performance in thin film transistors. We found that single crystal X-ray analysis, a standard characterisation technique for synthetic chemists, does not necessarily reveal the true nature of packing of such materials in thin films.

Results and Discussion

Thin film properties and morphology

We synthesised the three *N,N'*-dihydrotetraazapentacene derivatives **DHTA-X_2** through palladium catalysis.[24] The detailed synthesis procedure as well as the analytical data can be found in the supplementary information.

The synthesised materials are well soluble in organic solvents and exhibit individual optical absorption features due to their substitution pattern. The absorption and emission data of **DHTA** compounds are shown in Table S1 (see supplementary information). The Stokes shifts are always small, as expected for such rigid structures. The large optical gap is typical for compounds with the dihydropyrazine structure.[25,26] In the solid state, the fluorescence vanishes and the absorption features are slightly red shifted, 10 nm (431 cm^{-1}) for the unsubstituted **DHTA-H_2** and 23 nm (1044 cm^{-1} and 1058 cm^{-1}, respectively) for both the chlorinated (**DHTA-Cl_2**) and the fluorinated (**DHTA-F_2**) azaacenes.

We investigated the effect of choice of solvent on the microstructure of spin cast thin films by polarized microscopy (POM). The films of **DHTA-H_2**, **DHTA-Cl_2** and **DHTA-F_2** were deposited from xylene, mesitylene, or tetralin as they exhibit an increasing boiling point and should result in different film morphologies. Micrographs of images taken under cross-polarized light on polyimide are shown in Figure S2 in the supplementary information. In the case of unsubstituted **DHTA-H_2** and fluorinated **DHTA-F_2**, spherulitic growth is observed, while the chlorinated **DHTA-Cl_2** forms more irregular crystals. An increase in the solvent boiling point results in an increase in the domain size of the crystallites as the molecules have more time to organise during the evaporation process. This effect is surprisingly less distinct for **DHTA-Cl_2**, which appears to form similar morphologies independent of choice of solvent.

We investigated the microstructure of the films of the **DHTA-X_2** compounds by atomic force microscopy (AFM) (Figure 2). In the case of **DHTA-H_2**, we find an increase in the domain size of the films with increasing boiling point. Chlorinated **DHTA-Cl_2** forms flake-like crystals with a diameter ranging from 2-8 µm, regardless of choice of solvent. Films deposited from xylene exhibit slightly reduced grain size but appear denser.

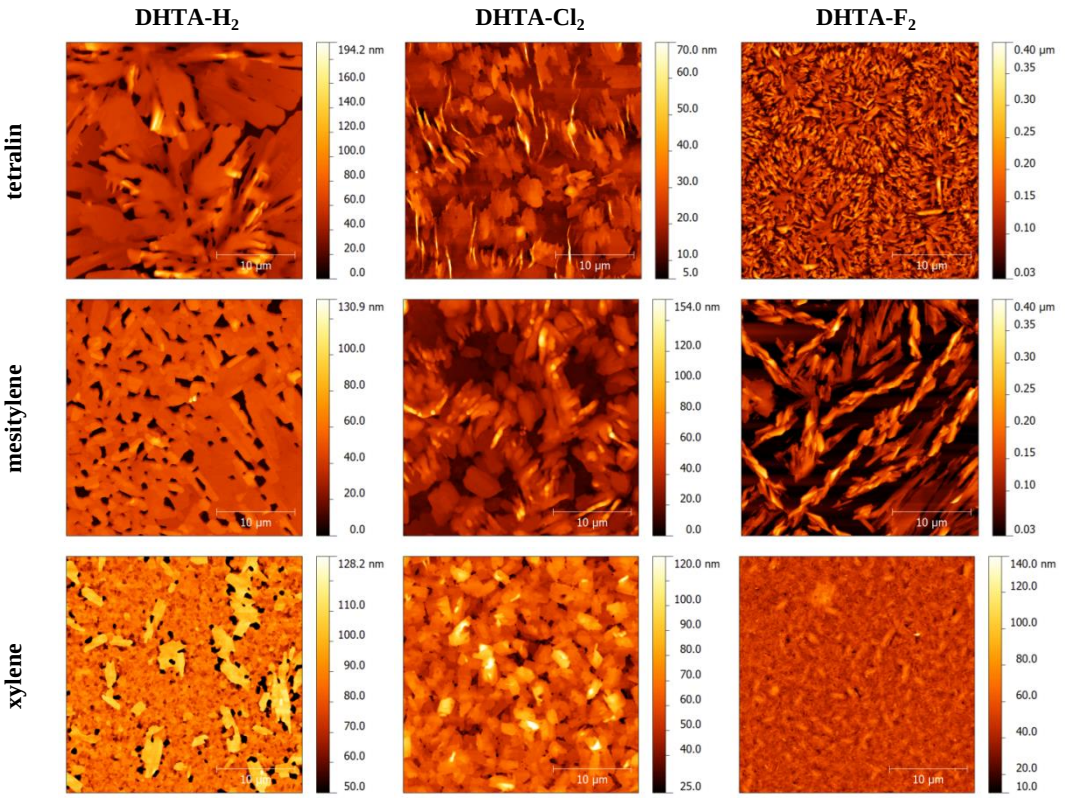

Fig. 2 AFM height images (30x30µm²) of the polycrystalline films of **DHTA-H_2**, **DHTA-Cl_2**, and **DHTA-F_2**. Spin-coated films on polyimide from tetralin, from mesitylene and xylene.

For each derivative, we measured the position of the highest occupied molecular orbital (HOMO) in spin-coated films by means of ultra-violet photoemission spectroscopy (Figure 3). We interpret the low binding energy edge of the valence band as the position of the HOMO of each of the three azaacenes **DHTA-X$_2$**. The influence of the substituents on the ionisation potential of the molecules in their solid state is significant. Chlorination stabilizes the HOMO of **DHTA-Cl$_2$** by 0.4 eV in comparison of that of the unsubstituated **DHTA-H$_2$**. The effect of the fluorine substituents is even greater (IP = 5.8 eV). These values are rather high for a traditional p-type semiconductor, however, reasonable hole injection from pentafluoro-benzenethiol (PFBT, pentafluorothiophenol) modified Au electrodes (work function 5.4 eV) can be achieved.[27]

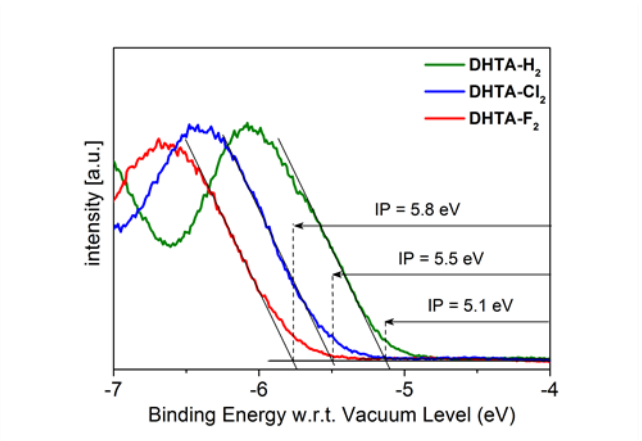

Fig. 3 UPS spectra of thin films show the increased ionisation potential due to halogenation with fluorine and chlorine respectively.

Thin film transistor performance

Figure 4 shows the top gate/ bottom contact transistor architecture we used to characterise the charge transport properties of our materials. The heteroacenes were spin cast from various solvents on top of the PFBT treated gold electrodes, structured by lithography onto a thin polyimide film. Perfluorinated Cytop polymer was used as dielectric, followed by a thermally evaporated Au gate. All NH-compounds resulted in working thin film transistors (TFT) with reasonable on-off ratios. Figure 4b shows the transfer and output characteristics for a TFT fabricated with an active layer of **DHTA-Cl$_2$** spin cast from xylene. Electrical characteristic curves for **DHTA-H$_2$** and **DHTA-F$_2$** are shown in Figure S3 and S4 in the supplementary information. Table 1 summarises the electrical parameters obtained for the various solvent/compound combinations. We show the best and the average values for the hole mobility calculated in the saturation regime. We note that the gate leakage in the devices is approximately one order of magnitude below the off current, showing that the on-off ratio is not dominated by the leakage in the device. The devices exhibit nearly no hysteresis, which indicates a well-defined and almost trap free interface with the dielectric polymer. The threshold voltages, obtained as intercept from a linear fit of the channel current in the saturation regime, are in the order of -10 to -20 V for all materials and do not follow a clear trend. The only exception to this are the TFTs fabricated from molecule **DHTA-H$_2$** in xylene, which suffer from an especially high off-current, therefore, the on/off-ratios as well as the average threshold voltage of +8V differ significantly from the other set of devices. The difluorinated material **DHTA-F$_2$** shows for all three solvents the lowest hole-mobilities with maximal values in the range of 10^{-4} cm²/V. The average hole mobility for the unsubstituted **DHTA-H$_2$** increases with the use of higher boiling point solvents and correlates with the observed increase of grain size in those films. Tetralin gives here the best performing TFTs with a hole mobility of up to 0.03 cm²/Vs. The transistors fabricated with DHTA-Cl$_2$ show the best hole mobilities ranging from 0.07 up to 0.11 cm^2/Vs. In excellent agreement with the morphology studies the average mobility remains stable at $4 \cdot 10^{-2}$ cm^2/Vs, independent of the boiling point of the solvent used for deposition.

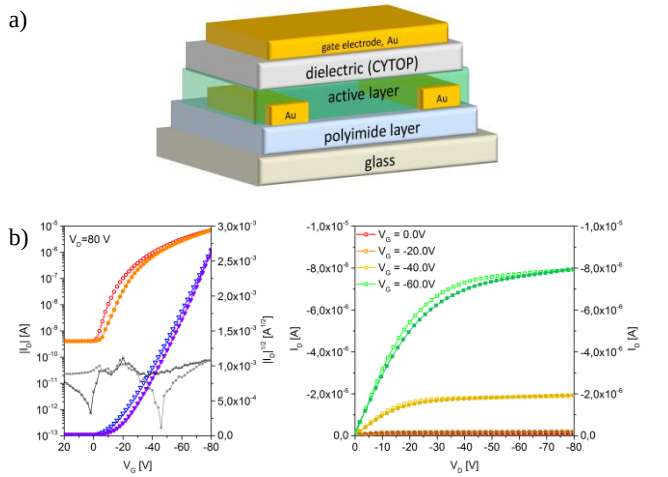

Fig. 4 a) Schematic cross section of the thin film transistors fabricated from **DHTA-X$_2$** derivatives as active semiconducting layer; b) transfer curves for a representative TFT of **DHTA-Cl$_2$** (W/L = 1000 µm / 20 µm, gate leakage in the background) at VSD = -80 V (left) and output characteristic (right).

X-Ray diffraction and crystal packing

To reveal the packing and to find the origin of the processing independent performance of **DHTA-Cl$_2$** we examined the three materials by X-ray structure analysis on the basis of single crystals grown in solution and X-ray diffraction patterns of their films. Single crystals of the three derivatives **DHTA** were obtained from solution to determine the packing of the molecules in the crystalline state (**Figure 5**). Detailed crystal parameters and .cif-files are listed in the supplementary information. Despite only small changes in their molecular structure, the packing patterns of **DHTA-H$_2$, DHTA-Cl$_2$** and **DHTA-F$_2$** differ significantly. **DHTA-H$_2$** stacks in isolated, one dimensional columns with a stacking distance of 3.44 Å of the aromatic cores of two neighbouring molecules (**Figure 5a**).[24] Such one dimensional structure would possible result

Table 1: Parameters of field-effect transistors with spin coated films of **DHTA-X_2** derivatives as active layer. All hole mobilities have been calculated in the saturation regime. The average value and standard deviation of the mobility μ_{hole} and threshold voltage V_{th} were obtained from a set of identical devices with different W/L-ratios.

Compound	solvent	μ_{hole} best [cm^2/Vs]	μ_{hole} average [cm^2/Vs]	threshold voltage average V_{th} [V]	on/off ratios
DHTA-H_2	tetralin	0.03	$(1.8\pm0.9)\cdot10^{-2}$	-(13 ±6)	10^4-10^5
	mesitylene	0.01	$(5.9\pm2.4)\cdot10^{-3}$	-(20.5±5)	10^4-10^5
	xylenes	0.005	$(1.4\pm1.6)\cdot10^{-3}$	(8±6)	10^2-10^3
DHTA-Cl_2	tetralin	0.09	$(4.3\pm2.7)\cdot10^{-2}$	-(23±6)	10^3-10^4
	mesitylene	0.07	$(3.0\pm1.9)\cdot10^{-2}$	-(20.5±4)	10^4
	xylenes	0.11	$(3.7\pm2.9)\cdot10^{-2}$	-(18±4)	10^3-10^4
DHTA-F_2	tetralin	$2.2\cdot10^{-4}$	$(7.3\pm5.9)\cdot10^{-5}$	-(11±7)	10^2-10^3
	mesitylene	$9.3\cdot10^{-3}$	$(1.5\pm3.5)\cdot10^{-3}$	-(29±7)	10^3-10^4
	xylenes	$8.5\cdot10^{-4}$	$(3.6\pm3.3)\cdot10^{-4}$	-(22±13)	10^3-10^4

in the formation of needle like crystals which is not observed in the AFM images (Figure 2), suggesting a different crystal packing (polymorph) in thin films. In **DHTA-Cl_2** pairs of molecules are arranged into a herringbone pattern (**Figure 5b**).[24] This packing motif has been observed previously for the analogue 5,14-bis(triisopropylsilylethynyl)pentacene in which the aromatic backbone also carries the side chains on the second aromatic ring.[6]

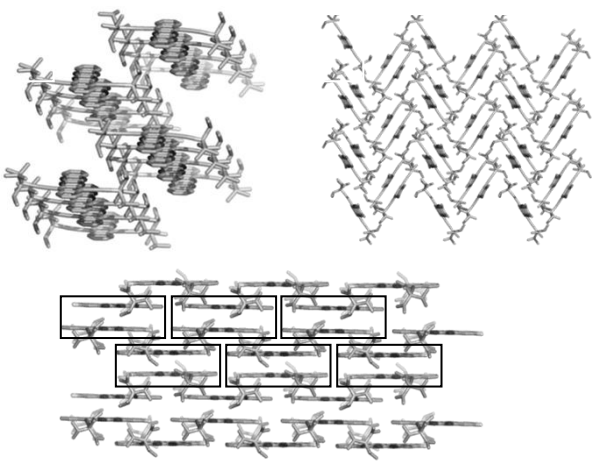

Fig. 5 Crystal packing of in solution grown crystals of **DHTA-H_2** (a), **DHTA-Cl_2** (b), and **DHTA-F_2** (c) in the solid state, while frames are included to highlight the dimeric structure of **DHTA-F_2** (randomly orientated cell axes to highlight the different packing motifs of each compound). All crystals were grown from hexane/toluene solutions.

The **DHTA-F_2** packs in a 'dimer-brickwall' motif. In each dimer, two fluorinated molecules are head-to-tail orientated with a π-π-stacking distance of 3.36 Å, minimizing their effective dipole moment. These dimers are packed in the brickwall motif (**Figure 5c**). **DHTA-F_2** exhibited a reversibly formed polymorph when the crystal was cooled to -73 °C (see SI). The packing and stacking of the aromatic units at low temperature differs only slightly from the described and shown polymorph which was measured at room temperature. All crystal structures show significantly bent TIPS-ethynyl side chains and express the energetic strain in each packing.

The spin cast films on polyimide from different solutions were then investigated with XRD to evaluate the orientation of the pentacene derivatives towards the substrate surface. In case of all three **DHTA** materials the XRD patterns could not be interpreted on the basis of the structures obtained in the single crystal analysis revealing the formation of new polymorphs in thin films. The observed diffraction patterns always show a similar background intensity ascribed to the glass/polyimide substrates (Figure 6 for xylene, for mesitylene and tetralin see Figure S5 in the supplementary information). The vast majority of the Bragg reflections can be understood as a series of higher order reflections {nh nk nl} where {hkl} constitutes the first-order reflection with a lattice spacing d_0 and where n is the integer-valued reflection order. Observation of these series of reflection implies for the employed Bragg-Brentano diffraction geometry that the corresponding lattice planes are parallel to the film surface. To obtain precise values for d_0, all diffraction patterns are height corrected. The Bragg-reflection always occurs at a diffraction angle 2θ of about 5°, which approximately corresponds to a d_0 = 17.5-18.0 Å.

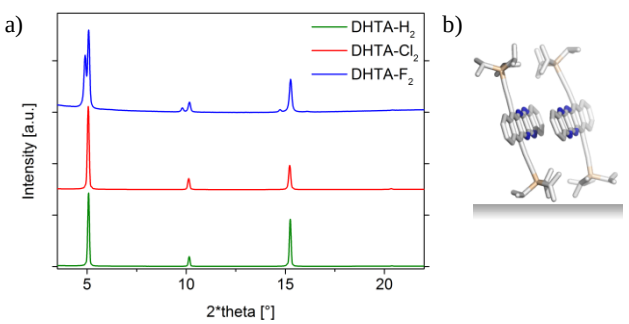

Fig. 6 a) X-Ray diffraction pattern of the films of **DHTA-H_2** (bottom), **DHTA-Cl_2** (middle) and **DHTA-F_2** spin cast from xylene solution. b) schematic orientation of the **DHTA** bodies towards the substrate surface.

This is in agreement of an edge-on orientation of the pentacene units, in which the TIPS-side chains face the substrate, well-known for TIPS-substituted pentacene derivatives.[28]

The investigated films of **DHTA-F_2** show two sets of higher-order reflections with similar d_0-values. The two series of reflections likely originate from two polymorphs of **DHTA-F_2** which both exhibit a lattice plane spacing of 18.02 Å and 17.39 Å. The higher d-spacing value could be correlated with the spacing of (h00) planes of the dimer brickwall packing motif found at room temperature for **DHTA-F_2** in the single crystal structure analysis (calculated d = 17.96 Å, found *via* XRD 18.02 Å). The second set of higher order reflexes must origin from a third polymorph, which we were unable to identify. The intensity ratio of the two different polymorphs for **DHTA-F_2** in the film changes upon the use of higher-boiling point solvents (see SI). This mixture of two different polymorphs might be the origin of the low FET performance and a problematic charge transport in this material. The thin films of **DHTA-H_2** and **DHTA-Cl_2** consist of a single polymorph with a lattice spacing of 17.42 Å and 17.45 Å, respectively. In both cases these reflections cannot be explained by the cell parameters and atomic structure obtained from the single crystal structure analysis. The Bragg reflections of films of **DHTA-H_2** and to some lesser extent those of **DHTA-Cl_2** show Laue oscillations, attributed to a homogenous film thickness.

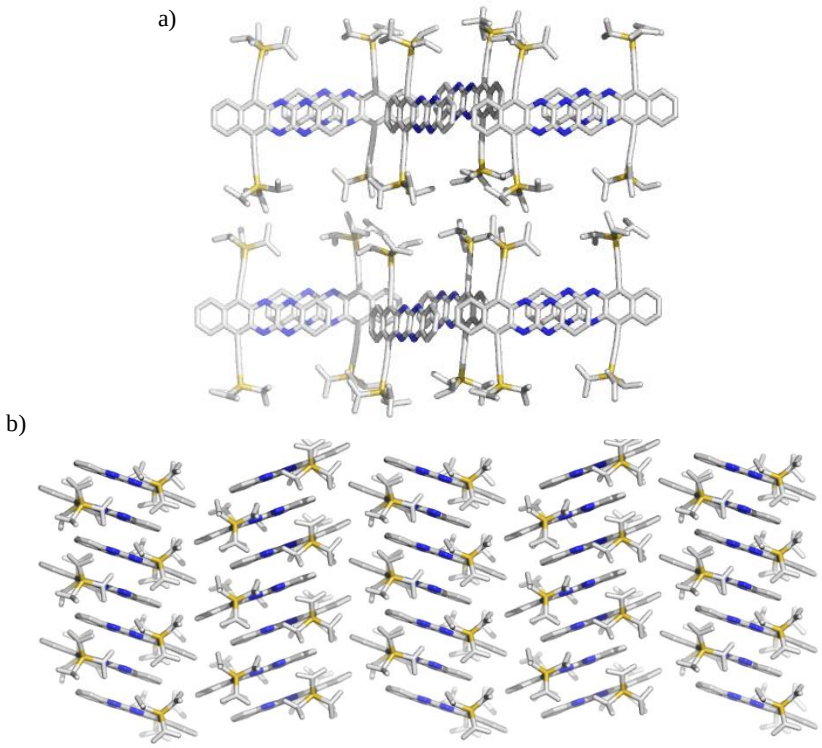

Fig. 7 a) Side view (horizontal a and b axes) of the film packing of **DHTA-H_2**, representing the layered structure of this material. b) Top view (almost along c* axis) of **DHTA-H_2**. This derivative packs in a zig-zag pattern in thin films. Crystals were grown on the substrate and dissected for a single crystal X-ray analysis.

To reveal the detailed packing and ordering of the pentacene units in the thin films, we tried to grow single crystals on polyimide substrate surfaces, i.e. similar to those during the film formation during spincoating. This succeeded in the case of **DHTA-H_2** by drop-casting **DHTA-H_2** from a xylene solution on a crystalline film on a polyimide substrate surface. Slow drying (as opposed to regular crystallization from solution in an open *glass* drum vial) conditions yielded crystal plates, carefully dissected from the surface and used for crystal X-Ray analysis. The important detail is that the crystals grow on the polyimide substrate. Single crystals of **DHTA-H_2** grown on the surface give a *new unit cell*. The pentacene units form in this polymorph a distinct, layered structure. Inside each layer the pentacene units form a zig-zag pattern of closely π-stacked aromatic cores with a π-π-distance of 3.34 Å (**Figure 7**). The observed XRD-reflections from the **DHTA-H_2** films and their observed intensities can be well related with the (00l) planes in which only the reflections for l=2n are present due to glide reflection symmetry of the crystal packing (calculated d-spacing 17.38 Å, XRD found 17.42 Å).

For the dihalogenated **DHTA-Cl_2** and **DHTA-F_2** similar crystallisation experiments were not successful. The exact packing of the pentacene units of **DHTA-Cl_2** remains unclear. But due to the similar d_0-spacing value and the similar intensity pattern of the film XRD diffraction patterns, we assume a significant similarity in the crystal structure of **DHTA-Cl_2** compared to **DHTA-H_2**.

Conclusions

We have synthesised three consanguine, laterally substituted *N,N'*-dihydrotetraazapentacenes and studied their film forming properties and microstructures. We revealed that those materials exhibit different polymorphous phases in thin films compared to solution grown single crystals. Study and analysis of a single crystal X-ray structures can be misleading. Based on our first impression the **DHTA** materials seemed to exhibit different solid state structures, but, once applied in thin films, their XRD-fingerprint is very similar, implying similar ordering. *N,N'*-dihydrotetraazapentacenes are attractive p-channel materials with robust, and for **DHTA-Cl$_2$** almost processing independent transistor performance for solution processed TFTs with hole mobilities up to 0.11 cm²/Vs.

Acknowledgements

F. Paulus thanks the Graduate College 'Connecting Molecular π-Systems into Advanced Functional Materials' for scholarship. U. Bunz and B. Lindner thank the DFG (Bu 771/7-1) for generous support.

Notes

[a] F. Paulus, B. Lindner, H. Reiß, Dr. F. Rominger, Prof. U. Bunz, Institute for Organic Chemistry, Ruprecht-Karls-University of Heidelberg, Im Neuenheimer Feld 270, 69120 Heidelberg, Germany, uwe.bunz@oci.uni-heidelberg.de

[b] Dr. A. Leineweber, Max Planck Institute for Intelligent Systems (formerly Max Planck Institute for Metals Research), Heisenbergstr. 3, 70569 Stuttgart, Germany[#]

[c] Prof. Dr. Y. Vaynzof, Kirchoff-Institute for Physics, Ruprecht-Karls-University of Heidelberg, Im Neuenheimer Feld 227, 69120 Heidelberg, Germany

[d] Prof. Y. Vaynzof, Prof. U. Bunz, Centre for Advanced Materials, Ruprecht-Karls-University of Heidelberg, Im Neuenheimer Feld 225, 69120 Heidelberg, Germany

[e] Prof. H. Sirringhaus Cavendish Laboratory, J J Thomson Ave., University Cambridge, Cambridge CB3 0HE, United Kingdom

[#] present address: Institute of Materials Science, Technische Universität Bergakademie Freiberg, 09599 Freiberg, Germany

† Electronic supplementary information (ESI) available: Synthesis of **DHTA** compounds and analytical data for **DHTA-F$_2$** (^{1}H-NMR, ^{13}C-NMR, IR, mass data, m.p.), optical properties of all **DHTA** compounds (absorption in film/solution, emission, stokes shift), images of polarized optical microscopy, additional I/V-characteristics, additional XRD data and crystal structures (.cif) and experimental details. For ESI and crystallographic data in CIF format see DOI: 10.1039/x0xx00000x

References

1. H. Klauk, *Chem. Soc. Rev.*, 2010, **39**, 2643–66.
2. H. Sirringhaus, *Adv. Mater.*, 2014, **26**, 1319–35.
3. G. R. Llorente, M.-B. Dufourg-Madec, D. J. Crouch, R. G. Pritchard, S. Ogier, and S. G. Yeates, *Chem. Commun. (Camb).*, 2009, 3059–61.
4. T. Sakanoue and H. Sirringhaus, *Nat. Mater.*, 2010, **9**, 736–40.
5. B. D. Naab, S. Himmelberger, Y. Diao, K. Vandewal, P. Wei, B. Lussem, A. Salleo, and Z. Bao, *Adv. Mater.*, 2013, **25**, 4663–7.
6. J. E. Anthony, J. S. Brooks, D. L. Eaton, and S. R. Parkin, *J. Am. Chem. Soc.*, 2001, **123**, 9482–3.
7. J. E. Anthony, *Chem. Rev.*, 2006, **106**, 5028–48.
8. J. E. Anthony, *Angew. Chem. Int. Ed. Engl.*, 2008, **47**, 452–83.
9. C. D. Dimitrakopoulos, a. R. Brown, and a. Pomp, *J. Appl. Phys.*, 1996, **80**, 2501.
10. D. J. Gundlach, T. N. Jackson, D. G. Schlom, and S. F. Nelson, *Appl. Phys. Lett.*, 1999, **74**, 3302.
11. C. C. Mattheus, G. a de Wijs, R. a de Groot, and T. T. M. Palstra, *J. Am. Chem. Soc.*, 2003, **125**, 6323–30.
12. D. Käfer and G. Witte, *Phys. Chem. Chem. Phys.*, 2005, **7**, 2850–3.
13. D. Käfer, L. Ruppel, G. Witte, and C. Wöll, *Phys. Rev. Lett.*, 2005, **95**, 166602.
14. Y. Diao, B. C.-K. Tee, G. Giri, J. Xu, D. H. Kim, H. a Becerril, R. M. Stoltenberg, T. H. Lee, G. Xue, S. C. B. Mannsfeld, and Z. Bao, *Nat. Mater.*, 2013, **12**, 665–71.
15. G. Giri, R. Li, D.-M. Smilgies, E. Q. Li, Y. Diao, K. M. Lenn, M. Chiu, D. W. Lin, R. Allen, J. Reinspach, S. C. B. Mannsfeld, S. T. Thoroddsen, P. Clancy, Z. Bao, and A. Amassian, *Nat. Commun.*, 2014, **5**, 3573.
16. G. Giri, S. Park, M. Vosgueritchian, M. M. Shulaker, and Z. Bao, *Adv. Mater.*, 2014, **26**, 487–93.
17. U. H. F. Bunz, J. U. Engelhart, B. D. Lindner, and M. Schaffroth, *Angew. Chem. Int. Ed. Engl.*, 2013, **52**, 3810–21.
18. U. H. F. Bunz, *Pure Appl. Chem.*, 2010, **82**, 953–968.
19. U. H. F. Bunz, *Chemistry*, 2009, **15**, 6780–9.
20. Q. Miao, T.-Q. Nguyen, T. Someya, G. B. Blanchet, and C. Nuckolls, *J. Am. Chem. Soc.*, 2003, **125**, 10284–7.
21. Q. Tang, D. Zhang, S. Wang, N. Ke, J. Xu, J. C. Yu, and Q. Miao, *Chem. Mater.*, 2009, **21**, 1400–1405.
22. Q. Tang, D. Zhang, S. Wang, N. Ke, J. Xu, J. C. Yu, and Q. Miao, *Chem. Mater.*, 2009, **21**, 1400–1405.
23. Z. He, D. Liu, R. Mao, Q. Tang, and Q. Miao, *Org. Lett.*, 2012, **14**, 1050–3.
24. O. Tverskoy, F. Rominger, A. Peters, H.-J. Himmel, and U. H. F. Bunz, *Angew. Chem. Int. Ed. Engl.*, 2011, **50**, 3557–60.
25. J. I. Wu, C. S. Wannere, Y. Mo, P. V. R. Schleyer, and U. H. F. Bunz, *J. Org. Chem.*, 2009, **74**, 4343–9.
26. S. Miao, S. M. Brombosz, P. V. R. Schleyer, J. I. Wu, S. Barlow, S. R. Marder, K. I. Hardcastle, and U. H. F. Bunz, *J. Am. Chem. Soc.*, 2008, **130**, 7339–44.
27. J. Chang, J. Li, K. L. Chang, J. Zhang, and J. Wu, *RSC Adv.*, 2013, **3**, 8721.
28. Y.-H. Kim, Y. U. Lee, J.-I. Han, S.-M. Han, and M.-K. Han, *J. Electrochem. Soc.*, 2007, **154**, H995.

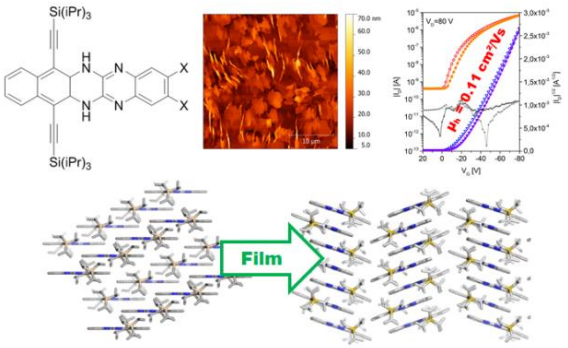

TOC / Key sentence: *N,N'*-dihydrotetraazapentacenes exhibit different polymorphs in spin cast thin films than in solution grown crystals and show interesting hole conducting properties with mobilities up to 0.11 cm^2/Vs.